

## 5.1A CAPABILITIES AND LIMITATIONS OF EISCAT AS AN MST RADAR

J. Rottger\*, M. Baron\*\*, K. Folkestad\*\*\*

\*EISCAT Scientific Association, Box 705, S-98127 Kiruna, Sweden

\*\*SRI International, 333 Ravenswood Avenue, Menlo Park, CA 94025

\*\*\*The Norwegian Defence Research Establishment, Box 25-N-2007, Kjeller, Norway

EISCAT is the European Incoherent Scatter radar facility established and operated by research institutions of Finland, France, W. Germany, Norway, Sweden, and the United Kingdom. Its facilities, which also can be used for coherent scatter research of the middle atmosphere, are located in Northern Scandinavia.

The observatory consists of two independent systems which will allow observations of the upper, middle and lower atmosphere: a tri-static UHF radar capable of vector drift measurements, and a monostatic VHF system. The geographic locations of the installations are shown in Figure 1. Ramfjordmoen, near Tromso, Norway, is the transmitter location for both systems. The additional receiver sites for the tristatic system are Kiruna, Sweden, and Sodankyla, Finland.

## TRANSMITTERS

The transmitter characteristics are shown in Table 1. Each is capable of CW or phase-coded pulses, in single- and multi-pulse sequences. The transmitted frequency can be changed from pulse to pulse or within a pulse, providing great flexibility in designing pulse codes.

Both transmitters employ klystrons as final power amplifiers: one tube in the UHF system and two tubes in the VHF system. The UHF system started its operation in summer 1981, but still has not yet reached its final reliability because of remaining transmitter problems. The VHF transmitter is still under construction. Since both systems are basically developed for ionospheric incoherent-scatter investigations, they are not yet too suitable for middle atmosphere investigations. Some modifications, such as fast T/R switching and short pulses, are feasible and shall be applied in future.

Because of the dual tube VHF configuration, the polarization of the transmitted signal may be easily changed by altering the phase relationship between the low-power RF signals driving the two klystrons.

## ANTENNAS

The UHF antennas (Table 2) are identical fully steerable parabolic dishes having Cassegrain feeds. The feed horn design is somewhat different at the transmitter site. A polarizer preceding the feed horn enables the transmitted/received polarization to be made circular, linear or elliptical to optimize the experimental arrangement (for a multi-static system, the optimum polarization is a function of site location and pointing angles). The polarizer settings are controlled by motor-driven phase changers.

With the narrow beam widths of the tristatic system, accurate pointing is essential in order to have the beams intersect in space. Small misalignments of each antenna's true pointing direction relative to the encoder readings are measured by systematic tracking of known radio stars. A model, fitted to the measurements, is used to correct the antenna pointing directions, also taking

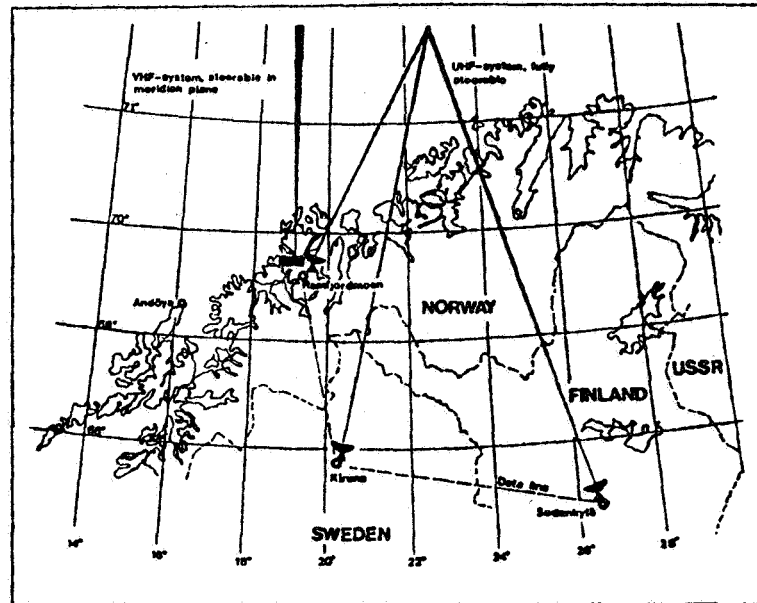


Figure 1. The EISCAT system in Northern Scandinavia.

Table 1 Characteristics of the EISCAT transmitters

	UHF	VHF
Frequencies	933.5 ± 3.5 MHz	224.0 ± 1.75 MHz
Frequency steps	0.5 MHz	0.25 MHz
Peak power	2 MW	5 MW
Average power	250 kW	625 kW
Pulse lengths	2 μs - 10 ms	10 μs - 1 ms
Pulse repetition frequencies	0 - 1000 Hz	0 - 1000 Hz
Maximum duty cycle	12.5%	12.5%

Table 2 UHF antenna specifications

Diameter of main reflector	32 m
Diameter of subreflector	4.6 m
Overall efficiency	0.65
Half-power beam width	0.6°
Gain	48 dB
Speed of mechanical movement	80°/min

into account tropospheric refraction, which is essential at low elevation angles.

The VHF antenna is a parabolic cylinder consisting of four identical 30 m x 40 m elements. The antenna may be operated in two modes. In mode I, the four elements are mechanically aligned and move together as one antenna. In this mode the antenna may radiate right or left circular polarization with the possibility of changing polarization from pulse to pulse or within a pulse. Linear polarization with the field  $\pm 45^\circ$  to the antenna axis may also be used. In mode II, the split-beam option, the four individual reflector elements act in pairs, producing two independent beams. Only left circular polarization is possible in this mode. By mechanical motion of the cylinder elements the beam can be steered  $30^\circ$  south and  $60^\circ$  north of the zenith in the meridional plane.

The VHF antenna is fed by a linear array of 128 crossed dipoles. The beam may be steered  $21^\circ$  from broadside by manually changing phasing cables to the dipoles. The VHF antenna is operational at the Tromso site and its characteristics are summarized in Table 3.

#### RECEIVERS

To minimize the system noise, the UHF front-end receivers are installed in instrument cabins immediately behind the feed horns of the antennas. At Kiruna and Sodankyla, helium-cooled parametric amplifiers are used, yielding an overall system noise temperature of about 40 K. At the transmitter site, the first stage of the receiver is an uncooled GaAs-FET amplifier, resulting in an overall system noise temperature of about 140 K.

The received signals are converted to an intermediate frequency of 120 MHz before being channelled to the main buildings for further down-conversion to 30 MHz second IF, filtering and processing.

The back-end receivers at each station consist of 8 channels for simultaneous reception of up to 8 transmitted frequencies. On each channel the signal is detected in quadrature. A complement of Bessel and Butterworth filters with several band widths is available.

The detected and filtered signals are fed to 8-bit A/D converters capable of independently sampling the 8 receiver channels at rates up to 500 kHz. If a phase-coded pulse is used, the samples are transferred to a decoder matched to a 13-bit Barker code. Otherwise, the decoder is bypassed and the samples passed directly to the correlator.

Table 3 VHF antenna characteristics

Orientation of plane of mechanical movement	$0.5^\circ$ west of north
Effective area in mode I, broadside:	
- Circular, calculated	$3250 \text{ m}^2$
- Horizontal, measured	$3330 \pm 240 \text{ m}^2$
- Vertical, measured	$2890 \pm 210 \text{ m}^2$
Beam widths, calculated for broadside:	
- Mode I	$0.6^\circ$ east/west $1.7^\circ$ north/south
- Mode II	$1.2^\circ$ east/west $1.7^\circ$ north/south
Range of steering in transit plane	$30^\circ$ south to $60^\circ$ north of zenith
Speed of mechanical movement	$5^\circ/\text{min}$

For the VHF system where the sky noise is 100-200 K, transistor amplifiers are sufficient for the receiver front-end. Otherwise, the receiving system is identical to the UHF one, except of different intermediate frequencies.

#### CORRELATORS

As described earlier, most of the information from the radar echoes is obtained from the spectrum. The same information, of course, is also contained in the complex autocorrelation function of the received signal. The EISCAT signal processing system is configured around a fast digital correlator. The correlator is a special purpose micro-programmable computer capable of handling the large number of multiplications and additions involved in calculating the complex correlation function. It operates at a clock-rate of 5 MHz and has a pipeline structure enabling parallel processing with a through-put rate of 50 Mega operations/sec. Its input buffer has 4 k memory for real and imaginary part. After calculation of the correlation function (ACFs), these can be integrated over software specified integration periods. The result memory covers 2 k words with 32 bit per real and imaginary part of the ACFs. Input buffer and result memory are extendable.

#### RADAR CONTROLLERS

All high-precision timing signals used to pulse control transmitter, receiver, ADC etc., are generated by a radar controller, one unit assigned to the VHF system and one at each site for the UHF radar. The central component is a 4 k word matrix of 2 x 16 words. Half of the matrix constitutes the "Instruction timetable", ITT, the other half the "Instruction table", IT. Each of the bits 0-13 is routed to a signal line having a particular control function in the transmit-receive operations. For instance, while the radar controller is in the transmit mode, defined by bit 14 being set, bit number 11 controls the RF modulation; the klystron beam is switched on upon setting of bit 12. The elements in the "dwell time array", ITT, determine how long (in  $\mu$ s) the corresponding instructions in the complementary array, IT, are to last.

The radar controller is programmed in a high-level language called TARLAN (Transmission And Receiver LAnguage). Instructions are transferred by the TARLAN compiler into a bit pattern corresponding to the IT and ITT tables which determine the state of the signal lines. The tables are then loaded, on command, from the sites' general purpose computer into the radar controller.

#### FREQUENCY AND TIMING STANDARDS

Because the EISCAT UHF radar is a pulsed tristatic system, timing at the three sites must be synchronized to within a few microseconds. For this purpose, each EISCAT station is equipped with a Cesium standard giving the frequencies 1, 5 and 10 MHz with an accuracy specified as  $10^{-11}$ . A fourth standard is available as a "travelling clock" for occasional comparison and adjustments. Long-term variations in the standards are corrected by noting the trend in long-term comparisons of the Cesium signals with Loran C signals received at 100 kHz from a transmitter in Vesteralen, Norway.

A real-time clock takes its input from the Cesium standard and feeds the radar controller with suitably shaped second-pulses. A provision is made in the clock for delaying the second-pulse in microsecond steps to compensate for long-term drifts in the standards and for the difference in propagation time

for the scatter volume to the different sites. The delay is computed and set by the routines governing the antenna pointing.

#### COMPUTERS AND INTER-SITE COMMUNICATION

At the transmitter station there is a Norsk Data NORD-10S computer with two 75 Megabyte discs. In addition, each station has a NORD-10 computer, having 128 k word memory, two 10 Megabyte discs and a standard complement of peripheral equipment, e.g., 1600 bpi tape drives. The standardized interfacing system CAMAC is used for interchanging data and control signals between the computer and the devices and processes which it serves. Permanent telephone lines operating at 9600 baud link the three site computers together, allowing for mutual transfer of programme routines and data. For scientific data analysis, EISCAT shares a larger computer, NORD 500, with the Kiruna Geophysical Institute.

#### ON-LINE DISPLAYS

Display software has been developed to use the on-site graphical terminals for real-time quick-look assessment of the quality of the received data. These displays have proved to be almost indispensable in supervising the operational states of the equipment during experiments. Options exist for plotting the complex autocorrelation functions, power spectra, and received signal as a function of range. All may be displayed with or without noise subtraction and for one of many range gates. The display also contains housekeeping information (e.g., time, antenna position) and system parameters (e.g., transmitted power and system temperature). Monitoring of operations at all three sites can be (sequentially) done from any one site through inter-computer transfer of the data.

#### REAL-TIME OPERATING SYSTEM

The EISCAT system, while performing experiments, is almost entirely computer controlled by EROS, which is the acronym for EISCAT's Real-time Operating System. To the user EROS appears as an assembly of high-level commands, about 75 altogether, for pointing antennas, setting the receivers, loading and controlling the correlators and the radar controllers, handling tapes and data transfer, activating and terminating real-time programmes and experiments. Using EROS in the remote mode at one station, one may control system parameters at one or both of the other two sites. This feature provides the possibility for supervising the operations at all three stations from one site.

A detailed technical description of the EISCAT facility can be found in an article by FOLKESTAD et al. (1983).

#### MIDDLE ATMOSPHERE OBSERVATIONS WITH THE EISCAT UHF RADAR

First stratosphere and mesosphere echoes were detected with the EISCAT UHF radar in summer 1982 after a special correlator program for coherent signals (pulse-to-pulse correlation) was prepared (Kofman, 1982). These experiments yielded basic experiences on the capabilities of the UHF radar for middle atmosphere research.

#### STRATOSPHERE

In contrast to incoherent scatter from the ionosphere, the stratosphere echoes are due to coherent scatter from clear air turbulence. Because of the not yet optimized transmit-receive switching, some limitations exist in the

monostatic mode when observing at short ranges. To records echoes from the stratosphere, the antenna has to be pointed at fairly low elevation angles below about  $20^\circ$ . Then problems arise because of ground clutter and shielding due to the mountains surrounding Tromso. The shielding also sets limits for bistatic observations. The elevation of the mountain ridges can be read from the horizon profile of Figure 2.

An example of stratospheric records is shown in Figure 3 which depicts a typical real-time display of autocorrelation functions (ACFs) and spectra for subsequent range gates. During this test operation on 3 August 1982, 2055 UT, the antenna pointed at  $17.4^\circ$  elevation and  $325^\circ$  azimuth. The transmitter was operated with 750 kW pulse peak power and 4% duty cycle. The pulse repetition rate was 1 ms and the pulse length 40  $\mu$ s. The first range gate was at 400  $\mu$ s, corresponding to 54 km (considering 40  $\mu$ s post-detection filter delay). This corresponds to the lowest sampled height at 16.4 km and a height resolution of 1.8 km. It evidently can be seen that receiver transition (saturation) effects occur out to range gate 2, corresponding to 440  $\mu$ s. This value obviously has to be improved in future experiments.

The records of Figure 3 clearly show evaluable echoes out to heights of about 22 km. The signal-to-noise ratio at this height is around 0 dB. Not too much signal power can be expected here because of the viscous subrange limitations discussed earlier. However, first test measurements in the bistatic mode prove that signals can be detected from maximum heights up to 30 km, because the Bragg wavelength is greater in this mode. This will allow measurements of vertical velocity and turbulence intensity up to the middle stratosphere.

The off-set of the power or Doppler spectra in Figure 3 proves that the signals are due to scatter from clear air turbulence carried by the background wind. This very clearly can be seen when operating the radar in the velocity-azimuth-display (VAD) mode, as shown in Figure 4. The change in sign of Doppler frequency when rotating the azimuth by  $180^\circ$  (upper diagrams) is obvious. Rotating the azimuth in steps of  $20^\circ$  and plotting the mean values of the spectra in the lower diagram of Figure 4 proves the expected sinusoidal variation. The mean wind speed of  $4 \text{ m s}^{-1}$  and direction from east, deduced from these radar data, is consistent with radiosonde wind data of Sodankyla.

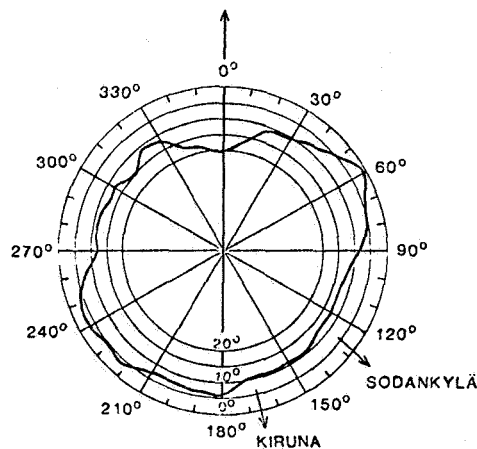


Figure 2. Horizon profile for the UHF transmitter at Tromso. The elevation scale extends from  $0^\circ$  to  $20^\circ$ .

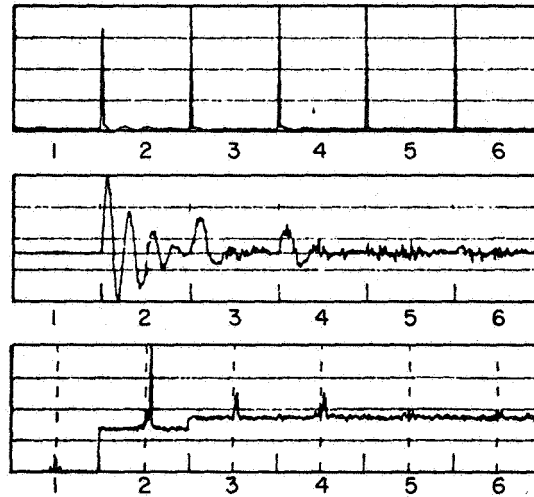


Figure 3. Autocorrelation functions (upper diagram: real part, center diagram: imaginary part) and power spectra (lower diagram) of stratosphere signals. Numbers denote range gates, corresponding to altitudes 16.4 (1), 18.2 (2), 20.0 (3), 21.8 (4), 23.6 (5) and 25.4 km. Receiver saturation is evident in range gates 1 and 2, signals disappear in gates 5 and 6. The ACFs were postintegrated over 30 s.

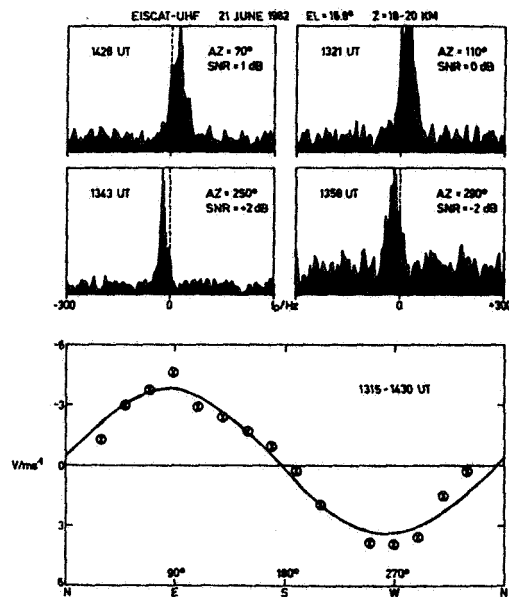


Figure 4. Spectra of stratosphere echoes (upper part), averaged over 30 s, and velocity-azimuth display in lower part.

## MESOSPHERE

Signals from mesospheric altitudes were also observed in the monostatic and bistatic mode. In an extended series of operations to support the rocket campaign CAMP (Cold Arctic Meso-Pause) at Esrange in July/August 1982, a fairly clear view on the occurrence frequency of these mesospheric echoes was obtained. Their appearance was mostly limited to a short duration up to some ten minutes, intense echoes often were connected with high absorption events recorded with riometers. It is fairly evident, therefore, that the mesospheric echoes are due to incoherent scatter from D-region ionization which was enhanced by high-energy particle precipitation. The comparison of the riometer reading and the average signal power (Figure 5), received from a scattering volume at 88 km altitude half the way between Tromso and Sodankyla, clearly indicates the correlation between these two measurements. Although an absolute calibration of the electron density in the probed volume is not yet done, it is found that the ionization had increased shortly by almost three orders of magnitude during the peak of the precipitation event.

The pulse-to-pulse correlation scheme allowed for the first time to measure the ion component spectra of these events (Figure 6). The signal-to-noise ratio was fairly low (-10 dB), but significant spectra were detected between 2135-2140 UT. In Figure 7 spectra-time intensity plots are shown which were obtained from monostatic observations at an elevation angle of 40°. The spectra exhibit a displacement when turning the antenna from south to west and v.v. This is caused by a wind, and the wind profile deduced from these data is consistent with mean circulation models. Since the spectra which are averaged over 10 s are each normalized to the peak power, these plots also indicate the signal-to-noise ratio. This obviously increased when the antenna turned to north, which is explained by a north-south gradient of the electron density in the D region. The spectral width is dependent on the temperature, collision frequency, and negative ion to electron ratio. Under model assumptions on two of these parameters, the remaining parameter can be deduced. By these means

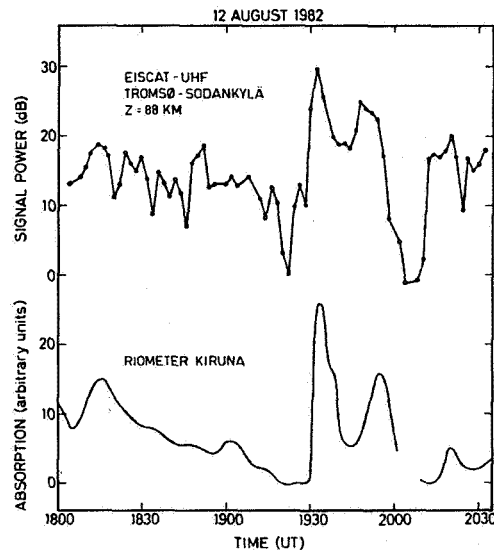


Figure 5. Incoherent-scatter signal power compared with riometer data.

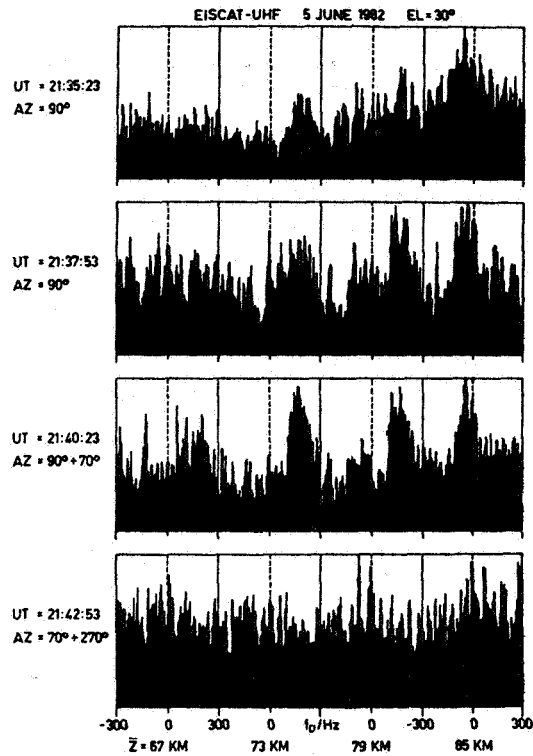


Figure 6. Spectra (2.5 min averages) of incoherent-scatter returns from the D region, obtained in the monostatic mode with 1.2 MW pulse peak power.

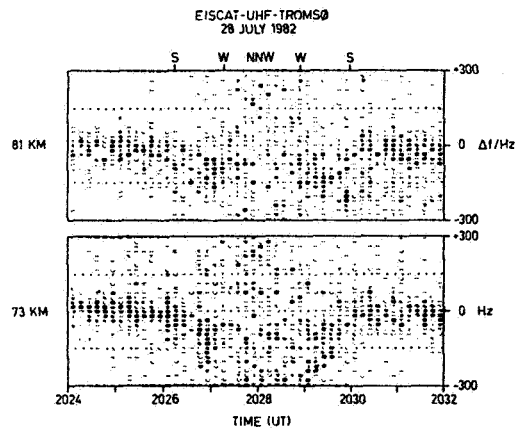


Figure 7. Spectra-time intensity plots of incoherent-scatter echoes. Between 2026 and 2030 UT the azimuth of the antenna was rotated, leading to a displacement and a disappearance of the spectra.

it may be possible to find indications on negative ions. In continuing these analyses, a unique chance exists to compare these EISCAT measurements with simultaneous in situ probes by rockets flown during the CAMP campaign.

#### CONTRIBUTIONS TO FUTURE RESEARCH OF THE M.A.

The analysis of about 60 hours of middle atmosphere observations in 1982 leads to the conclusion that EISCAT's capabilities to measure mesospheric parameters will improve during moderately or strongly disturbed conditions. It then will be possible to measure profiles (with height resolution down to about 1 km) of wind velocity, electron density, and temperature/collision frequency. It also should be possible in some instances to determine ion masses. The accuracy of these partly interdependent estimates will strongly improve by having available information on temperature or collision frequency and ion mass from other experiments. Of course, observations of these parameters in the lower thermosphere (90-130 km) are possible with EISCAT even under fairly undisturbed conditions. The steerability of the UHF system will allow to measure the geographical distribution of some scalar parameters within some 100 km distance around Tromsø.

By recording in the monostatic VAD mode (velocity-azimuth display), stratospheric wind velocities up to the maximum height of 24 km can be recorded. In the bistatic mode, echoes from stratospheric heights up to about 30 km can be received and estimates of the vertical velocity and turbulence refractive index constant can be deduced.

More details on experiments to investigate the middle atmosphere with EISCAT and the interpretation of coherent and incoherent scatter echoes are discussed in a paper by ROTTGER (1983).

The EISCAT Scientific Association is funded and operated by Suomen Akatemia/Finland, Centre Nationale de la Recherche Scientifique/France, Max-Planck-Gesellschaft/W. Germany, Norges Naturvitenskapelige Forskningsrad/Norway, Naturvetenskapliga Forskningsradet/Sweden and Science and Engineering Research Council/United Kingdom.

(References in this paper are included in the Publications listed below).

#### PUBLICATIONS RELATED TO EISCAT MST CAPABILITIES

- Folkestad, K., T. Hagfors and S. Westerlund (1983), EISCAT - an updated description of technical characteristics and operational capabilities, Radio Sci., 18, 867-879.
- Kofman, W. (1982), A mesospheric experiment: measurement scheme and program implementation, EISCAT Techn. Note 82/35, EISCAT-HQ, Kiruna, Sweden.
- Kofman, W., F. Bertin, A. Crenieu, J. Rottger and P. J. S. Williams (1983), The EISCAT Mesospheric Measurements during the CAMP Campaign, IAMAP/IAGA Symposium during IUGG Assembly, Hamburg, August 1983.
- Rottger, J. (1983), The use of the EISCAT radar facility for middle atmosphere research, Proc. 6th ESA Symposium on European Sounding-Rocket and Balloon Research (to be published).
- Rottger, J. (1983), Some capabilities of the EISCAT UHF radar for investigation of the stratosphere, Preprint Volume 21th Conference on Radar Meteorology, (in press).